JPP Journal of Pharmacy and Pharmacology

JPP 2007, 59: 51–57

Received February 2, 2006
Accepted October 2, 2006
DOI 10.1211/jpp.59.1.0007
ISSN 0022-3573

Image analysis by pulse coupled neural networks (PCNN)—a novel approach in granule size characterization

Osmo Antikainen, Kyriakos Kachrimanis, Stavros Malamataris, Jouko Yliruusi and Niklas Sandler

Abstract

A biologically inspired spiking neural network model, the pulse coupled neural network (PCNN), has been applied for the first time in bulk particle characterization, and specifically in the characterization of pharmaceutical granule size distributions. The PCNN was trained on surface images of pharmaceutical granule beds, and the adjustable parameters (radius neuron interconnection, r_0, linking weight coefficient, β, local threshold potential, V_Θ, and number of iterations) were successfully optimized using design of experiments. As demonstrated with size fractions of granules, it was found that the PCNN produced granule size-dependent signals. In general, a first highest and relatively narrow peak located in the region of two to twelve iterations corresponded to smaller particle size, while larger particles resulted in wider peaks and in highest (not first) peak at a range between 13 and 25 iterations. Better predictions, i.e. lower RMSEP (root mean squared error of prediction) values, were obtained using high β value, low r_0 and V_Θ values, while the number of iterations had to exceed 110 and the optimized model (RMSEP lower than 5) corresponded to PCNN variables: $r_0 = 1$, $\beta = 0.4$, $V_\Theta = 2$, and number of iterations = 150. The coefficient of determination (R^2) of the model was 0.94 and the predicted variation (Q^2) was 0.91, while the Pearson correlation coefficient between the predicted and the measured mean particle size by sieving for eight test batches was 0.98. These findings could be characterized as promising and encouraging for the further use of image analysis by PCNNs in pharmaceutical bulk particle size and shape characterization.

Division of Pharmaceutical Technology, Faculty of Pharmacy, University of Helsinki, Finland

Osmo Antikainen, Jouko Yliruusi, Niklas Sandler

Department of Pharmaceutical Technology, School of Pharmacy, Aristotle University of Thessaloniki, Greece

Kyriakos Kachrimanis, Stavros Malamataris

School of Pharmacy, University of Otago, Dunedin, New Zealand

Niklas Sandler

Correspondence: N. Sandler, AstraZeneca R&D, Pharmaceutical and Analytical R&D, Material Sciences Group, Laboratory Block, Silk Road Business Park, Charter Way, Macclesfield, Cheshire SK10 2NA, UK. E-mail: niklas.sandler@astrazeneca.com

Funding and acknowledgements: The authors wish to thank M. Sc. students Hanna Tervakoski and Johannes Pietiläinen for technical assistance with the surface imaging. Financial support for the project "New image analysis methods in drug development" from the Jenny and Antti Wihuri Foundation is acknowledged. The Academy of Finland and Finnish Cultural Foundation are also thanked for financial support (N. Sandler)

Introduction

Images are produced with optical and other techniques, and consequently handled with various methods after suitable image processing and used for numerous purposes. In pharmaceutical manufacturing, photographs or digital versions of images based on electron scanning, on atomic force measurement or on photometry are used after suitable analysis (image analysis) for evaluation of surface roughness and morphology of uncoated and coated particles (tablets, pellets, granules and crystals), as well as for particle sizing and shape description (Brewer & Ramsland 1995; Eriksson et al 1997; Kennedy & Niebergall 1997; Andrès et al 1998; Andersson et al 2000). Other methods used for particle size measurement, e.g. sieving, Coulter counter and laser diffraction, cannot provide evaluation of shape and surface roughness which besides size have significant effects on handling of dosage forms (tablets, granules, pellets) and on the processability of pharmaceutical particulate materials, such as powders and suspensions. Grasa & Abanades (2001) have pointed out the growing importance of obtaining solid concentrations from digitalized images in industries handling bulk powders. Efforts to overcome limitations in image analysis and to develop more useful applications of automated microscopy have been made within powder technology, and lately the number of commercial off-line, in-line and on-line image analysis instruments has increased.

However, limitations in routine use of image analysis methods for particle characterization exist and they are usually related to the relative slowness of the characterization process, the large size of an image as a dataset and the great variety of methods that can be chosen for overcoming these problems (Pons et al 1999). Ros et al (1997) have stated that

the characterization of granular products with image analysis is complex because of difficulty in the definition of the sample size, of need for sample dispersion and because of data diversity that may be extracted from digital images. Particularly in particle size and shape analysis only characteristics of individual particles may be considered and the feature extraction procedure applied is of great importance. Most of the aforementioned limitations can be overcome by considering the use of a key attribute of a bulk particulate material, which is a typical pattern of the field-of-view image called texture. Texture is related to the distribution of the spatial variation in gray scale levels of monochrome images and can be connected to general bulk-particle characteristics (Bonifazi 1997). Therefore, global measurements of the texture that is observed in an image can portray information about the particle size. Smaller particles form a finer texture and larger particles display coarser textures. An advantage of textural methods is that particles do not have to be identified individually.

Recently, suggestion of novel image processing approaches for more efficient image feature extraction has followed the development of the "mammalian visual cortex models" after progress in understanding of the visual cortex function in the mammalian (cat's) brain-region that receives information from the eye. Particularly, the Pulse Coupled Neural Network (PCNN) algorithm was developed that uses similar means as the biological eye to extract essential information from images and besides has self organizing abilities. It simulates the neural activity in the cat's visual cortex and results in image-pulses created from an original image (Eckhorn et al 1990). Furthermore, improved applications of PCNN have been reported. Lindblad & Kinser (1998) listed the different approaches where PCNN was used including smoothing of noisy images, segmentation, texture identification and edge detection of images. Johnson & Padgett (1999) reviewed the applications and implementations of PCNN thoroughly. Kinser et al (2000) applied pulse image analysis with three-dimensional chemical structural data and found it useful in studies of structure property relationships. Åberg & Jacobsson (2001) also utilized the PCNN successfully in three-dimensional quantitative structure–retention relationship modelling. The PCNN was also used effectively in satellite image analysis (Waldemark et al 2000) and medical image processing (Keller & McKinnon 1999). In previous reports, we have shown that examination of pharmaceutical powders as larger populations by employing undispersed samples through processing surface images after forming beds or columns can be advantageous (Laitinen et al 2000, 2002, 2003). A new optical imaging set-up was proposed and means to derive a descriptive parameter of size and shape (grey scale difference matrix) from undispersed granule surface images was suggested employing multivariate modelling. This approach is considered as advantageous because it removes the problems related to sample dispersion, which often constitute the most problematic stage. Finally, combination of this approach with new tools suggested for effective compression of image information may be advantageous for substantial image edge and texture feature information for the case of pharmaceutical particulate material e.g. in the analysis of particle size and shape characteristics for screening of pharmaceutical granulations.

In this study a novel neural network approach related to mammalian visual cortex models has been evaluated for image feature extraction, exploiting surface images of packed pharmaceutical granules. PCNN was used to create image signatures that were one-dimensional feature vectors and they functioned as fingerprints for images of different fractionated and unfractionated granules produced with fluidized bed granulation. The image signature vectors obtained were then linked to size distribution data by employing multivariate modelling.

Materials and Methods

Materials

Thirty-four different batches of granulations were used, which were obtained by applying a fluidized bed method under altered process conditions (Laitinen et al 2004). The granulations were deliberately planned to produce different kinds of mean particle sizes and size-distribution profiles to be able to establish a relationship between PCNN spectra and real particle size distributions. The particle size distributions were measured with sieve analysis (10 min with amplitude 6) employing a vibratory sieve shaker (Analysette 3pro, Fritsch, Oberstein, Germany) and the following twelve sieves: 0.045, 0.071, 0.090, 0.125, 0.160, 0.250, 0.355, 0.500, 0.710, 1.000, 1.400, and 2.000 mm. The sample size for sieve analysis was 50 g and the results of weight proportions were derived employing the "autosizer" program. Also, sieve fractions of these granulations were used as a test set to demonstrate the effect of size on PCNN spectra. The sieve fractions were seven, namely: 0.125–0.160, 0.160–0.250, 0.250–355, 0.355–500, 0.500–0.710, 0.710–1.000, 1.000–1.400 mm.

Imaging

Images of granule batches (unfractionated and fractionated) were taken with a surface imaging unit with a slightly modified procedure of that described by Laitinen et al (2003, 2004), which is described below. A fixed volume of granulations was poured in a quartz sample cuvette (dimensions: height 2 cm, breadth 1.2 cm) and tapped to give a completely covered area against the cuvette wall. Images of three sample replicas were taken ($n = 3$). The imaging unit consisted of a light source and a monochrome CCD camera (JAI, CV-M50, Copenhagen, Denmark) with a resolution of 576×768 pixels and a lens objective, which was connected to a frame grabber (WinTV, Hauppauge Computer Works, Hauppauge, NY) and a Personal Computer running MatLab Image Acquisition Toolbox (MatLab 6.5.1, Mathworks, Norwick, USA). The light source was accurately positioned to light laterally the imaging area and cast shadows on the surface. The image of the sample cuvette was taken from a horizontal direction. The illumination system included one lamp-housing, 50 W quartz tungsten halogen lamp and a collimating lens assembly (Oriel Instruments, Stratford, CT). A 50-mm lens objective and an additional 40-mm extension tube were used. The distance

from the sample was 20 cm. The angle of illumination was 30° and the used power source voltage was 5.5 V. The dimensions of the imaged area were 8 × 10 mm, and one pixel represented squares of approximately 10-μm side length. All images were taken in a dark room with no disturbing light sources. The calibration of the imaging conditions was made through a program written for MatLab which controlled the brightness of the images.

Pulse Coupled Neural Network (PCNN) selection

PCNN is a very simplified network of a single layer with local lateral connections between neurons. The PCNN neuron (Eckhorn neuron) is composed of multiple nodes which form a grid, i.e. a 2 D-vector. Furthermore, the nodes are coupled with their neighbours within a radius r_0. The indices (*i,j*) indicate each individual node in the grid (Bečanović 2000). The Eckhorn neuron consists of a number of compartments, which include two input compartments, a linking, L, and a feeding, F compartment (Figure 1). The network gets stimuli by both feeding and inhibitory linking. The linking and feeding signals are combined in an internal activation system, which builds up the signals until they exceed a dynamic threshold. When this threshold is exceeded the network fires an output signal, the membrane voltage, U. The membrane voltage is then compared with a local threshold, Θ (Lindblad & Kinser 1998). The output alters the threshold and the linking and feeding neurons signals. The PCNN uses an image as input, where each pixel is used as input to one neuron. The output from each neuron is either one or zero indicating whether it spikes or not. This output in question is then sent back to the neuron itself and its neighbouring neurons. The spiking means that neurons fire in synchrony in homogenous areas associated in the input image. One of the natural features of the PCNN is the fact that local interconnections between neurons exist. Neurons have a tendency to fire in groups making segmentation and edge detection possible in the image, while the iterative nature of PCNN makes the groupings break up after several iterations (Figure 2). This break-up is dependent on the textural information and allows evaluation of the image's texture by the PCNN. After a finished cycle the PCNN generates a time series-like one-dimensional vector (Figure 2), which serves as a "fingerprint" of the input matrix (the source image) and can be used for its classification (Johnson 1994). A full mathematical description of PCNN was given by Lindblad & Kinser (1998). The algorithm is performed by continuous iterations of the input and output, and most important equations behind PCNN are:

$$F_{ij}[n] = e^{-\alpha F} F_{ij}[n-1] + V_F \sum M_{ijkl} Y_{kl}[n-1] + S_{ij}, \quad (1)$$

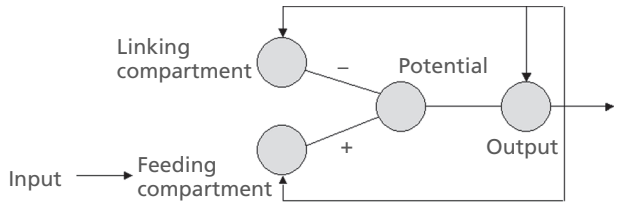

Figure 1 Simplified PCNN pulse neuron.

$$L_{ij}[n] = e^{-\alpha L} L_{ij}[n-1] + V_L \sum W_{ijkl} Y_{kl}[n-1], \quad (2)$$

$$U_{ij}[n] = F_{ij}[n]\,(1 + \beta L_{ij}[n]), \quad (3)$$

$$Y_{ij}[n] = 1 \quad \text{if} \quad U_{ij}[n] > \Theta_{ij}[n-1], \text{ and 0 otherwise} \quad (4)$$

$$\Theta_{ij}[n] = e^{-\alpha\Theta} \Theta_{ij}[n-1] + V_\Theta Y_{ij}[n], \quad (5)$$

$$G[n] = \sum Y_{ij}[n]. \quad (6)$$

In these equations S is the input stimulus i.e. the pixel intensity in (*i,j*) position on the grid. It is computed from the pixel intensity (i + k, j + l), in the pixel with coordinates (x,y). F is the feeding and L is the linking compartment of the neuron. There are three potentials or normalizing constants, V_L, V_F and V_Θ, for the linking, feeding and local threshold, respectively. αF, αL and $\alpha\Theta$ are time constants for feed, link and dynamic threshold, respectively. M and W are the constant synaptic weights and they are dependent on the distance between neurons. Y stands for the output of the neuron and it gets either the binary value 0 or 1. Θ is the dynamic threshold, U is the internal activation of the neuron, and Θ is the linking weight parameter. The one-dimensional time signal or spectra is computed as a global array, G. During the cycle, the internal activity and the output of every neuron is updated after any iteration. This is done on the basis of a stimulus signal of the used image and the preceding state of the network.

Modelling and evaluation of models

The settings of the PCNN parameters are of great significance when training the network for a certain task. The amount of parameters to control and handle is the main weakness of the PCNN according to Bečanović (2000). However, typically only a few parameters have to be adjusted to reach optimal settings for a certain problem. Relevant studies have been carried out by Székely & Lindblad (1998), but most often parameters have to be adjusted by trial and error to work in an explicit way (Bečanović 2000). The use of an experimental design study to find out optimal settings is obviously a rational approach, as it is shown in this, as well as previous, studies (Åberg & Jacobsson 2001). Recently researchers have focused on simplifying PCNNs e.g. by developing adaptive parameter determination (Bi et al 2004; Gu et al 2004a, b).

In this study all calculations to produce PCNN time signals were performed using the PCNN image processing toolbox for Matlab, freely available under a GNU general public license (details can be requested from the authors). The following standard parameters were used for the sieved size fractions: $r_0 = 3$ (radius), $\beta = 0.2$ (linking coefficient), $V_F = 0.01$, $V_L = 1$, $V_\Theta = 2$, decay constants $\alpha L = 1$, $\alpha\Theta = 10$ and $\alpha F = 0.001$. The choice of parameters tested was based on suggestions in the available literature, while all other settings were set as explained previously. In total, 2754 PCNN time signals were produced (34 batches of granulations × 27 different PCNN settings × 3 replicate images). The relation between the PCNN

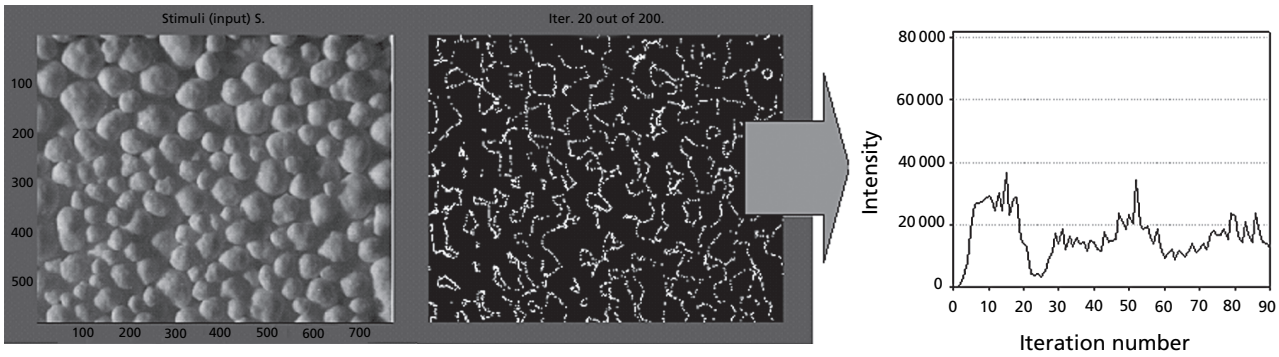

Figure 2 Left: a stimulus (input) image. Middle: a pulse image output after 20 iterations in which particle edges can clearly be detected. Right: final output, a time signal created by the PCNN.

time signals and the particle size distribution (weight proportion on twelve sieves) was modelled by partial least squares (PLS) regression, using the Simca version 10.5 software (Umetrics AB, Sweden). PLS relates two data matrices, X and Y, to each other by a multivariate model. In this study X was the PCNN time signal and Y was the sieve analysis results. The PCNN time signals were used as explanatory variables and the percent mass proportion of the measured 12 sieve fractions were used as the response variables. As a result we received a 12-fraction particle size distribution calculated from one image. This size distribution could then be used for calculating other particle size parameters e.g. the mean particle size.

For the training set granule batches, a 3^3 experimental design matrix was used to investigate the relevance of different settings of the PCNN calculations and to find which values produced the best PLS model. The three levels of r_0 used were 1, 3 and 5, the levels of β were 0.1, 0.2 and 0.4, and the levels of V_θ were 2, 10 and 20. The 27 different combinations of PCNN settings were evaluated using batches R1, R6, R9, R20, R21, R23, R30 and R31 as a test set, on the basis of the RMSEP (root mean squared error of prediction) values of the PLS models, calculated as follows:

$$RMSEP = \sqrt{\frac{\sum (y_p - y_r)^2}{n}} \tag{8}$$

where y_p is the predicted value for each size fraction, y_r the measured value for each size fraction and n is the number of experiments. Multilinear stepwise regression analysis was used to study the dependence of response variable (RMSEP) on the r_0, β and V_θ values of the eight-batch test set, using the Modde software (Modde for Windows, v. 3.0, Umetri AB, Sweden). The best model was selected to be used in calculation of particle size distributions from the test set images.

Results and Discussion

Dependence of PCNN time signal and particle size

Figure 3 shows the surface images for four different sieve fractions of granules together with the respective PCNN time signals. They clearly exemplify the size dependency of the time signals. In general, a first highest relatively narrow peak located in the region of two to twelve iterations corresponds to smaller particle size. Larger particles result in wider peaks, in general, and in highest (not first) peak at a range between 13 and 25 iterations. In other words, the time signals are more pulse-like for smaller particles, i.e. reach high acute angled peaks and return almost to zero, whereas with increasing particle size the pulsation shows smaller variation. Further size related differences of the time signals may be evaluated using Principal Component Analysis, but such an approach was considered out of the scope of this study.

Optimization of PCNN parameters

The mean RMSEP values calculated from the three replicate images of each of the eight test set batches varied between 2.5 and 8.5 (Table 1). The overall RMSEP value of the test set for each created model was used in the regression modelling. Test set granulations with a mean particle size between 250 and 450 μm had lower RMSEP values probably because batches with a similar mean particle size (and size distribution) were predominant (Table 2). Higher RMSEP, ranging from 5 to 8.5, were found for batches whose particle size range was under represented in the model, such as R23 (mean particle size 586 μm) and R9 (1185 μm). Therefore, a larger number of granulations representing coarser particle sizes would obviously be important for creation of enhanced models in future studies. The relationships between the response

Table 1 The particle mean size values for predicted (by the PCNN model) vs observed (measured with sieving)

Batch	Predicted (mm) ± s.d.	Observed (mm) ± s.d.
R1	0.390 ± 3.2	0.416 ± 6.9
R6	0.248 ± 4.3	0.239 ± 2.8
R9	1.085 ± 23.0	1.185 ± 17.0
R20	0.468 ± 3.4	0.350 ± 5.2
R21	0.288 ± 2.3	0.316 ± 9.1
R23	0.656 ± 34.0	0.586 ± 69.2
R30	0.310 ± 7.2	0.289 ± 11.9
R31	0.268 ± 5.4	0.280 ± 10.3

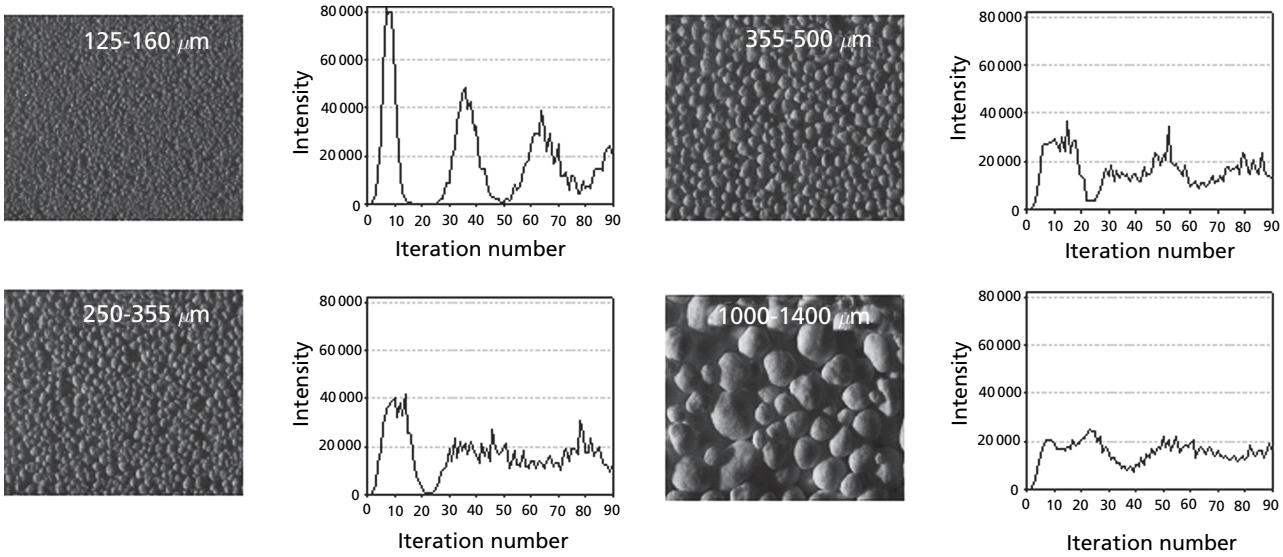

Figure 3 Examples of PCNN time signals for four different sieve fractions (size range indicated on the image) exemplifying the particle size dependency of the PCNN output. The corresponding time signal is situated on the right side of each image.

Table 2 Mean particle size of the fluidized bed granulations experimentally determined by sieve analysis.

Batch	Particle mean size (μm) ± s.d.
R1	416 ± 6.9
R2	1147 ± 44.5
R3	622 ± 15.2
R4	260 ± 9.2
R5	266 ± 7.2
R6	239 ± 2.8
R7	1413 ± 202.0
R9	1.185 ± 17.0
R10	241 ± 3.6
R12	246 ± 5.8
R13	282 ± 6.3
R14	273 ± 2.7
R15	289 ± 1.0
R16	331 ± 5.5
R17	390 ± 3.2
R18	293 ± 8.8
R19	412 ± 25.1
R20	350 ± 5.2
R21	316 ± 9.1
R22	276 ± 70.3
R23	586 ± 69.2
R24	592 ± 76.6
R25	603 ± 21.8
R26	223 ± 7.2
R27	616 ± 14.3
R28	237 ± 11.4
R29	557 ± 39.7
R30	289 ± 11.9
R31	280 ± 10.3
R32	356 ± 25.0
R34	233 ± 7.2
R35	294 ± 3.9
R36	295 ± 4.8

Batches R8 and R11 were unsuccessful granulations and were therefore not presented.

variable (RMSEP) and the number of iterations, as well as between RMSEP and the values of the adjustable parameters (r_0, β and V_Θ) obtained by the multilinear regression modelling showed clear trends in optimal PCNN parameters to be used. In summary, within the tested range, the use of high β value and low r_0 and low V_Θ values gave better models, i.e. lower RMSEP values. Regarding the number of iterations it has to be above 110 to acquire the best model. This is in agreement with the findings of Åberg & Jacobsson (2001), who also developed a PLS model for 3D molecular images and the PCNN spectra, and found that the predictive ability of their model increased from 40 to 110–130 iterations. A contour plot presenting the combined effects of V_Θ and number of iterations for the higher β value (0.4) and the lower r_0 value (1), Figure 4, shows clearly that the best model (RMSEP lower than 5) may be obtained with a V_Θ value lower than 2.5 and when the number of iterations is between 140 and 178. This finding may be explained by the tendency of small V_Θ values to synchronize regions, whereas larger V_Θ values spread spikes apart (Lindblad et al 1997). Also, it is in agreement with the finding of Åberg & Jacobsson (2001), who reported that when V_F was too large, compared with V_Θ, the neurons were able to spike several times in a row and the segmentation ability of the PCNN was degraded.

Prediction of granule size and size distribution from PCNN spectra

The model with the optimal PCNN variables giving the best overall response in RMSEP values was chosen to be used in particle size and size distribution measurement of granules. The PCNN settings of the chosen model were: $r_0 = 1$ (radius), $\beta = 0.4$ (linking coefficient), $V_\Theta = 2$, and number of iterations = 150. The coefficient of determination (R^2) of the model was 0.94 and the predicted variation (Q^2) was 0.91.

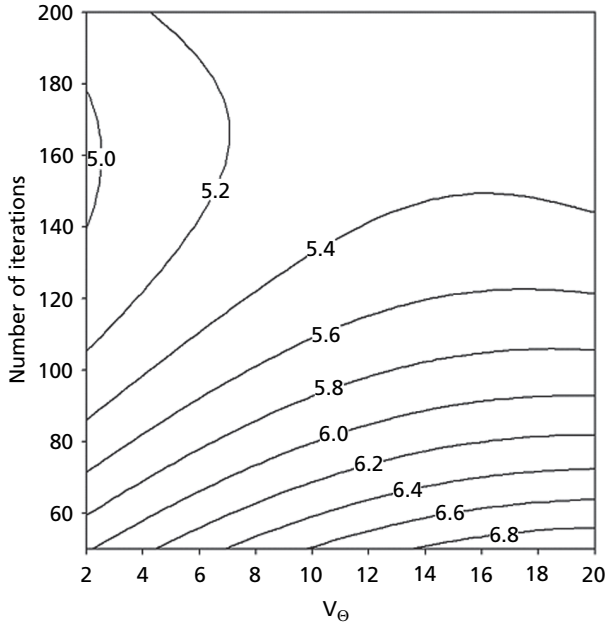

Figure 4 Contour plot presenting the combined effects of V_Θ and number of iterations on the response variable (RMSEP), for the higher β value (0.4) and the lower r_0 value (1).

The predictive power was calculated according to cross-validation. The Pearson correlation coefficient between the predicted and the measured mean particle size by sieving of the eight test batches was 0.98 (Table 1).

Taking into consideration that for quantitative measurements the creation and the inspection of the imaged surface in a controlled and reproducible manner is very important, this study shows that PCNN can be used to form textural fingerprints for surface images, which then can be used in sizing of particles. The results obtained can be characterized as promising and encouraging for the further use of image analysis by PCNNs in pharmaceutical bulk particle size and shape characterization. Feasible areas of study can be found in measurement of particle morphology including shape and roughness and this is also justified by the effort of many researchers to establish suitable automated systems and to design digital and optical hardware.

Conclusions

This first attempt of PCNN for use in bulk determination of particle size and size distribution based on textural fingerprints of surface images demonstrated its feasibility for pharmaceutical granules. The PCNN adjustable parameters may be successfully optimized using standard design of experiment methodology. The PCNN produced granule size-dependent time signals. In general, a first highest and relatively narrow peak located in the region of two to twelve iterations corresponded to smaller particle size, while larger particles resulted in wider peaks and in highest (not first) peak at a range between 13 and 25 iterations. Better predictions, i.e. lower RMSEP values, were obtained using a high β value and low r_0 and V_θ values, while the number of iterations had to exceed 110 and the optimized model (RMSEP lower than 5) corresponded to PCNN variables: $r_0 = 1$ (radius), $\beta = 0.4$ (linking weight coefficient), $V_\Theta = 2$ (local threshold potential), and number of iterations = 150. The coefficient of determination (R^2) of the model was 0.94 and the predicted variation (Q^2) was 0.91, while the Pearson correlation coefficient between the predicted and the measured mean particle size by sieving for eight test batches was 0.98. These findings can be characterized as promising and encouraging for the further use of image analysis by PCNNs in pharmaceutical bulk particle size and shape characterization.

References

Åberg, K. M., Jacobsson, S. P. (2001) Pre-processing of three-way data by pulse-coupled neural networks: an imaging approach. *Chemom. Intell. Lab. Syst*. **57**: 25–36

Andersson, M., Holmquist, B., Lindquist, J., Nilsson, O., Wahlund, K.-G. (2000) Analysis of film coating thickness and surface area of pharmaceutical pellets using fluorescence microscopy and image analysis. *J. Pharm. Biomed. Anal*. **22**: 325–339

Andrès, C., Bracconi, P., Réginault, P., Blouquin, P., Rochat, M. H., Pourcelot, Y. (1998) Assessing the particle size of a broadly dispersed powder by complementary techniques. *Int. J. Pharm*. **167**: 129–138

Bečanović, V. (2000) *Signal and image processing in engineering physics*. Ph. D. Thesis, The Royal Institute of Technology (KTH), Stockholm

Bi, Y. W., Qiu, T., Li, X., Guo, Y. (2004) Automatic image segmentation based on a simplified pulse coupled neural network. *Proc. Advances Neural Networks* **3174**: 405–410

Bonifazi, G. (1997) Particulate solids control in bulk by image analysis. *Proc. Powder Bulk Solids Conference*. Rosemont IL, May 5–8, pp 337–348

Brewer, E., Ramsland, A. (1995) Particle size determination by automated microscopical imaging analysis with comparison to laser diffraction. *J. Pharm. Sci*. **84**: 499–501

Eckhorn, R., Reitboeck, H. J., Arndt, M., Dicke, P. (1990) Feature linking via synchronization among distributed assemblies: simulations of results from cat visual cortex. *Neural Comp*. **2**: 293–307

Eriksson, M., Alderborn, G., Nyström, C., Podczeck, F., Newton, J. M. (1997) Comparison between and evaluation of some methods for the assessment of the sphericity of pellets. *Int. J. Pharm*. **148**: 149–154

Grasa, G., Abanades, J. C. (2001) A calibration procedure to obtain solid concentrations from digital images of bulk powders. *Powder Technol*. **114**: 125–128

Gu, X. D., Zhang, L. M., Yu, D. H. (2004a) Equivalence relation between PCNN and mathematical morphology in image processing. *J. Computer-Aided Design Computer Graphics* (Chinese) **16**: 1029–1032

Gu, X. D., Zhang, L. M., Yu, D. H. (2004b) Simplified PCNN and its periodic solutions. *Proc. Advances Neural Networks* **3173**: 26–31

Johnson, J. L. (1994) Pulse-coupled neural nets: translation, rotation, scale distortion and intensity signal invariance for images. *Appl. Opt*. **33**: 6239–6253

Johnson, J. L., Padgett, M. L. (1999) PCNN models and applications. *IEEE Transactions Neural Networks* **10**: 480–498

Keller, P. E., McKinnon, D. (1999) Pulse-coupled neural networks for medical image analysis. *Proceedings of SPIE: The International Society for Optical Engineering* **3722**: 444–451

Kennedy, J. P., Niebergall, P. J. (1997) Preliminary assessment of an image analysis method for the evaluation of pharmaceutical coatings. *Pharm. Dev. Technol*. **2**: 205–212

Kinser, J. M., Waldemark, K., Lindblad, T., Jacobsson, S. P. (2000) Multidimensional pulse image processing of chemical structure data. *Chemometrics Intelligent Laboratory Systems* **51**: 115–124

Laitinen, N., Antikainen, O., Mannermaa, J.-P., Yliruusi, J. (2000) Content-based image retrieval: a new promising technique in powder technology. *Pharm. Dev. Technol*. **5**: 171–179

Laitinen, N., Antikainen, O., Yliruusi, J. (2002) Does a powder surface contain all necessary information for particle size distribution analysis? *Eur. J. Pharm. Sci*. **17**: 217–227

Laitinen, N., Antikainen, O., Yliruusi, J. (2003) Characterization of particle sizes in bulk pharmaceutical solids using digital image information. *AAPS PharmSciTech*. **4**: article 49

Laitinen, N., Antikainen, O., Rantanen, J., Yliruusi, J. (2004) New perspectives for visual characterization of pharmaceutical solids. *J. Pharm. Sci*. **93**: 165–176

Lindblad, Th., Kinser, J. M. (1998) Image processing using pulse-coupled neural networks. *Perspectives in neural computing*. Springer-Verlag Limited, London

Lindblad, Th., Becanovic, V., Lindsey, C. S., Szekely, G. (1997) Intelligent detectors modelled from the cat's eye. *Nucl. Intr. Methods* A **389**: 245–250

Pons, M. N., Vivier, H., Belaroui, K., Bernard-Michel, B., Cordier, F., Oulhana, D. Dodds, J. A. (1999) Particle morphology: from visualisation to measurement. *Powder Technol*. **103**: 44–57

Ros, F., Guillaume, S., Bellon-Maurel, V., Bertrand, D. (1997) Building and preprocessing of image data using indices of representativeness and classification applied to granular product characterization. *J. Chemom*. **11**: 469–482

Székely, G., Lindblad, T. (1998) Parameter adaptation in a simplified pulse-coupled neural network. *Proceedings of VI-DYNN*. 98 SPIE, Vol. 3728

Waldemark, K., Lindblad, T., Becanovic, V., Guillen, J. L. L., Klinger, P. L. (2000) Patterns from the sky-Satellite image analysis using pulse coupled neural networks for pre-processing, segmentation and edge detection. *Patt. Recogn. Lett*. **21**: 227–237